Solar Phys (2007) 240: 135–151
DOI 10.1007/s11207-006-0197-z

Streamer Belt and Chains as the Main Sources of Quasi-Stationary Slow Solar Wind

M. Eselevich · V. Eselevich · K. Fujiki

Received: 4 April 2006 / Accepted: 12 November 2006 / Published online: 24 February 2007

Abstract Synoptic maps of white-light coronal brightness from SOHO/LASCO C2 and distributions of solar wind velocity obtained from interplanetary scintillation are studied. Regions with velocity $V \approx 300-450$ km s^{-1} and increased density $N > 10$ cm^{-3}, typical of the "slow" solar wind originating from the belt and chains of streamers, are shown to exist at Earth's orbit, between the fast solar wind flows (with a maximum velocity $V_{\max} \approx 450-800$ km s^{-1}). The belt and chains of streamers are the main sources of the "slow" solar wind. As the sources of "slow" solar wind, the contribution from the chains of streamers may be comparable to that from the streamer belt.

1. Introduction

"Quasi-stationary solar wind" (SW) is a term for plasma streams whose sources on the Sun exist for a sufficiently long period — for more than one day, often weeks and even months. It constitutes an aggregate of primarily two types of plasma streams with distinct properties: the "slow" SW (maximum velocity 450 km s^{-1} or lower) originating in the coronal streamer belt, and the "fast" SW (maximum velocity, correspondingly, exceeding 450 km s^{-1}) flowing out of coronal holes (CH) or associated open magnetic tubes (OMT) (see, *e.g.*, Eselevich, Kaigorodov, and Fainshtein, 1990; Schwenn and Marsch, 1991; McComas, Elliott, and von Steiger, 2002).

The coronal streamer belt, with "slow" SW flowing inside, separates regions in the corona with different polarity of the radial component of the magnetic field (*e.g.*, Svalgaard, Wilcox, and Duvall, 1974; Korzhov, 1977; Gosling *et al.*, 1981; Burlaga, Hundhausen, and Zhao, 1981; Wilcox and Hundhausen, 1983). Thus a neutral line of the Sun's global magnetic field runs within and along the streamer belt.

M. Eselevich (✉) · V. Eselevich
Institute of Solar-Terrestrial Physics, Irkutsk, Russia
e-mail: esel@iszf.irk.ru

K. Fujiki
Solar-Terrestrial Environment Laboratory, Nagoya University, Toyokawa, Japan

Apart from the streamer belt itself, there are its branches called "chains of streamers" (Eselevich, Fainshtein, and Rudenko, 1999). Like the streamer belt, the chains appear in the form of areas with increased brightness in white-light coronal images. A "slow" SW with nearly the same properties as the one in the streamer belt flows in the chains. Chains differ from the belt, however, in that, in the corona, they separate magnetic tubes with identical polarities of magnetic field. Therefore, the calculated structures of the magnetic field have the form of a single arch in the streamer belt and double arches in chains of streamers (Eselevich, Fainshtein, and Rudenko, 1999). On the whole, the properties of chains of streamers have been little investigated, and this terminology has not been universally adopted. Thus, in the literature (Eselevich and Fainshtein, 1992; Eselevich, 1995; Eselevich and Tong, 1997), they were first called a "heliospheric current sheet without a neutral line" (HCS without an NL); while in Zhao and Webb (2003), they were called a "unipolar closed field region" (the streamer belt itself was called a "bipolar closed field region"). In Ivanov *et al.* (2002), manifestations of chains in the heliosphere were termed "subsector boundaries". We will use the term "chains of streamers".

Segments of the streamer belt and chains in the corona have enhanced brightness. This results from plasma density in these structures being several times as high as the surrounding plasma density. Such segments with enhanced brightness may be observed in the corona both at low and high latitudes (near a solar activity maximum).

The solar wind velocity V has been measured chiefly for near-equatorial portions of the streamer belt. At distances $R = (4-6)R_0$ (R_0 is the solar radius), the velocity is about $V \approx 50-100$ km s^{-1} (Sheeley *et al.*, 1997; Tappin, Simnett, and Lyons, 1999; Eselevich, Fainshtein, and Eselevich, 2000; Strachan *et al.*, 2002), while at Earth's orbit $V \approx 300-450$ km s^{-1} (Borrini *et al.*, 1981). Measurements from Ulysses (Smith *et al.*, 1993) at distance $R = 4.7$ AU recorded individual parts of the slow SW with $V \approx 400-450$ km s^{-1} corresponding to streamer belt portions at latitudes no larger than 30 degrees.

Interplanetary scintillation (IPS) measurements may answer the question concerning the SW velocity in the streamer belt in high latitudes. A tomographic analysis (Kojima *et al.*, 1998) makes it possible to obtain velocity synoptic maps at the source surface ($R = 2.5R_0$) for individual Carrington rotations. These maps are created based on IPS observations covering from 0.2 to 1 AU. Comparison of such maps with Fe XIV line intensity distributions, as well as with calculated coronal magnetic field under the potential-field approximation, has shown that, in some cases, the slow SW may be associated with small-sized coronal holes (Kojima *et al.*, 1999; Ohmi *et al.*, 2004). Even a brief examination of velocity synoptic maps reveals, however, that, near a solar activity maximum, the slow SW occupies a noticeably greater area than the total area of individual small coronal holes and the streamer belt. One of possible reasons for such a discrepancy may be the neglect of chains of streamers, in which the slow SW flows as well.

Analysis of the streamer belt based on coronal images from LASCO C2 coronagraph (Brueckner *et al.*, 1995) has shown the presence of ray structures with increased brightness (Eselevich and Eselevich, 1999). Such structures undergo considerable (up to 30 – 40 degrees) deviations from the radial direction in the direction normal to the plane of the streamer belt, within distances $R \approx (1-3)R_0$ from the center of the Sun. At distances $R \geq (3-4)R_0$, ray structures of the streamer belt and chains generally do not suffer appreciable deviation in latitude (Eselevich and Eselevich, 2002). Hence there is a real opportunity to find sources of the slow SW by comparing positions of the streamer belt and chains at distances $R \geq (3-4)R_0$ found from LASCO C2 white-light coronal images to synoptic velocity maps based on IPS data.

At the orbit of Earth, the SW flowing in the streamer belt and chains differs greatly from SW from coronal holes in terms of such properties as plasma density N (Borrini *et al.*, 1981), mass flux $j = NV$, the O^{7+}/O^{6+} abundance ratio reflecting the coronal temperature, and the Mg/O ratio controlled by the FIP effect (Geiss, Gloeckler, and von Steiger, 1995). Entropy in the form $S = k \ln(T/N^{0.5})$ is a reliable parameter to distinguish these two types of streams. Here, in the formula for entropy, the polytropic index is assumed $n = 1.5$. Hereafter, following Burton *et al.* (1999), instead of entropy S, we will use its argument $T/N^{0.5}$ under the logarithm. A sharp difference between the above parameters appears to testify to different origins of these streams.

The goal of this work is to find sources on the Sun of quasi-stationary slow SW with increased density and decreased entropy by comparing two-dimensional SW velocity distributions on the source surface ($R = 2.5R_0$) found from IPS data to synoptic coronal brightness maps from LASCO C2.

2. Data

The following are the main data used for the analysis:

1. Synoptic maps of coronal brightness in white light at a fixed distance from the center of the Sun constructed according to LASCO C2 data. The C2 coronagraph gives images of the corona at $R = (2-6)R_0$.
2. OMNI2 data on the SW parameters having one-hour time resolution, National Space Science Data Center, as well as WIND solar wind data.
3. Neutral line position of the radial component of the Sun's global magnetic field as calculated under potential-field approximation by J.T. Hoeksema (http://quake.stanford.edu/~wso).
4. The solar wind velocity distributions on the source surface ($R = 2.5R_0$) in the form of synoptic maps for individual Carrington rotations obtained by the tomographic analysis of IPS data (Solar-Terrestrial Environment Laboratory, Nagoya University).

3. Method of Analysis

We determined positions of the streamer belt and chains using brightness contours of the white-light corona measured on one of the limbs. In doing so, we used the following assumptions based on previous observational studies: The streamer belt is a layer of finite thickness (of the order of 5 degrees in the heliographic coordinate system) completely surrounding the Sun. Chains of streamers are isolated parts of the layer which do not surround the entire Sun and have properties similar to the streamer belt (Eselevich, Fainshtein, and Rudenko, 1999). The ends of the chains are positioned either in the nearest sections of the streamer belt or in the neighboring chains. The SW plasma density in the belt and chains may be several times as high as the outside density. In addition, density may vary noticeably (at a given distance R) along the belt and chains, and change with time in their different parts independently. The streamer belt and chains can be identified as a sequence of brightness maxima in a synoptic map of coronal brightness. These maxima are connected by "bridges" also having an increased, but to a somewhat lesser extent, brightness. Drawing lines over brightness maxima and "bridges", we obtain the position of the belt and chains of streamers. In doing so we were guided by the following rules: (a) A chain should have at least one

reliable part with increased brightness having the length of half or more of the full length of the chain; (b) A chain begins and ends in the nearest sections of the streamer belt or other chains; (c) We draw a monotonic curve representing the invisible part of the chain to connect it to the streamer belt or to other chains.

The reliability of this method was repeatedly inspected against the streamer belt, whose position usually coincides fairly well with the position of a calculated neutral line (NL). A comparison with the position of the neutral line also allows the areas with increased brightness corresponding to the streamer belt to be distinguished from those due to chains of streamers.

At high latitudes, it is often difficult to determine on which — the visible or invisible — side of the Sun the observed chain is situated. To determine this, we compared its location with the position of sufficiently stable large coronal holes. A high-latitude chain that coincides with coronal hole areas was considered to have its base on the back side of the Sun. Information on the position of CHs was obtained from daily maps of coronal holes in the He I line (ftp://ftp.noao.edu/kpvt/daily/lowres/).

The parts of streamer belt and chains intersecting the ecliptic plane were used to validate their positions determined in a synoptic map. For this purpose, these parts were compared with their manifestations in the solar wind data at Earth's orbit. In doing so, we took into account the following conditions (Eselevich and Fainshtein, 1992):

1. The part of the streamer belt stands out by its increased density $N > 10$ cm^{-3} and by the presence of a sector boundary within it. In other words, the azimuth angle φ of the magnetic field has an odd number of changes and therefore the dominant sign of the interplanetary magnetic field (IMF) is different on each side of that part.
2. The part of the chain of streamer also has an increased density $N \geq 10$ cm^{-3} but does not contain a sector boundary. An azimuth angle has an even number of changes and the dominant IMF sign is the same on each side of that part.

Both these parts of the slow SW are characterized by a decreased entropy argument $T/N^{0.5}$ (Burton *et al.*, 1999).

The analysis method as a whole constituted the following series of operations:

1. Coronal brightness maps at $R \geq (3-4)R_0$, made separately from the E- and W-limb data, were used to determine positions of the belt and chains of streamers, taking into account the calculated neutral line location.
2. Thus obtained positions of the belt and chains were superimposed on the synoptic maps of SW velocity on the source surface according to IPS data.
3. To validate the positions of the belt and chains we compared their parts intersecting the ecliptic plane with the SW parameters at Earth's orbit.

The arrival time T_{orb} to Earth's orbit of a given intersection point of the belt or chains with the ecliptic plane near the Sun were determined from the formula (Fainshtein, 1999):

$$T_{\text{orb}} \approx T_0 + \left(4.6 \times 10^4\right)/V \ \left(\text{km s}^{-1}\right). \tag{1}$$

Here T_0 is the instant of time when the given intersection point passes the central meridian. The expression $(4.6 \times 10^4)/V$ (in hours) is the transit time from the Sun to Earth of the slow SW that has velocity V (in km s^{-1}) at 1 AU. According to Eselevich and Eselevich (2005), the condition $V \approx 350$ km s^{-1} is met at Earth's orbit with an accuracy of several tens of km s^{-1}. Therefore the transit time was supposed to be 5.5 days everywhere.

4. Two-Dimensional Distributions of SW Velocities According to IPS Measurements Compared to White-Light Coronal Brightness from LASCO C2

As discussed above, the belt and chains of streamers appear as a series of areas with increased brightness in a synoptic map of coronal brightness in white light. The streamer belt differs from the chains in that it is much closer to the calculated NL of the magnetic field.

Figures 1 and 2 show examples of how positions of the belt and chains of streamers are found for rotation CR1976 (May 6 – June 2, 2001) — from brightness data in the E and W limbs, respectively. For convenience, brightness in synoptic maps is shown as contours. The brighter regions in the corona correspond to the darker shaded regions. On the E limb, positions of the belt and chains are shown by thin lines; on the W limb, by thick lines. The chains are shown by dashed lines, the streamer belt by a solid line. Position of the calculated neutral line is shown as a curve of asterisks. For comparison convenience, all curves (belt and chains of streamers, as well as NL) are plotted on the same synoptic map without brightness contours (Figure 3).

One can see that in the left part of the map, the positions of the streamer belt derived from the coronal brightness data of the E (Figure 1, thin solid line) and W limbs (Figure 2, thick solid line) are in close agreement with the position of the neutral line (the curve of asterisks). In the right part of the map, agreement with the calculated curve is worse, even though the general run of the curves is similar. It can be argued that all these curves on the synoptic map (one calculated and two observed) fluctuate around a certain average curve — the "carcass" which is nearly invariable during a Carrington rotation. Deviations of each of these curves from the average curve in particular places can reach $\pm(10-60)$ degrees in both longitude and latitude. The main causes of these deviations are probably as follows:

1. The NL position is inaccurate due to uncertainty in calculating the coronal magnetic field under potential-field approximation.

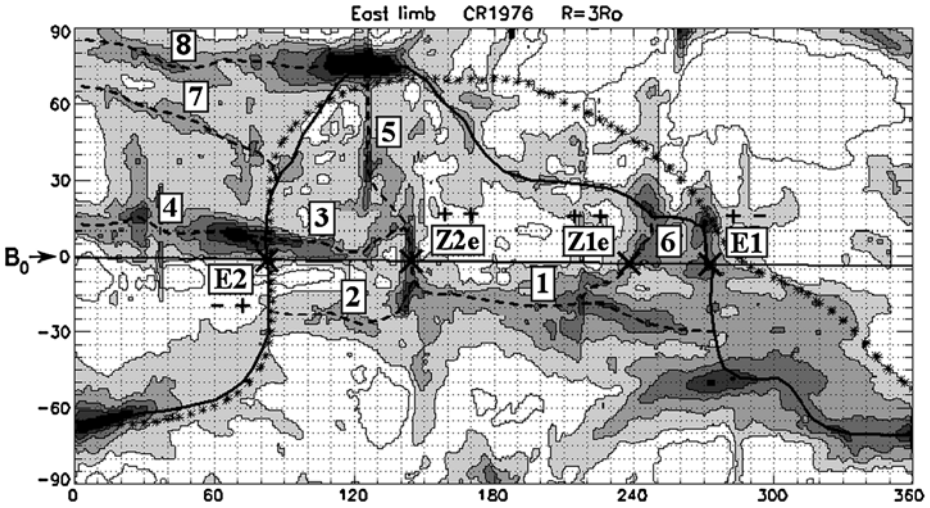

Figure 1 Contours of white-light coronal brightness on a synoptic map, made from LASCO C2 data for the E limb, $R = 3R_0$, CR1976. The asterisks are the calculated NL (courtesy J.T. Hoekzema), the solid curve is the streamer belt, and the dashed curves are chains of streamers. The "+" and "−" signs show the polarity of the Sun's global magnetic field. The solid horizontal line is the latitude B_0 of the solar disk center.

2. A finite thickness of the streamer belt and variations of brightness in some parts may lead to errors in determining the position of the belt.
3. The time evolution of the belt during a Carrington rotation may lead to slightly different positions of the belt as obtained from the observations on the E and W limbs.

When drawing chains of streamers we kept in mind that, for CR1976 (Figures 1 and 2), a stable polar coronal hole was absent at latitudes higher than 70 degrees in the northern hemisphere, in the longitude range 0 – 120 degrees, but there was a stable CH at high latitudes in the southern hemisphere in the longitude range 120 – 180 degrees.

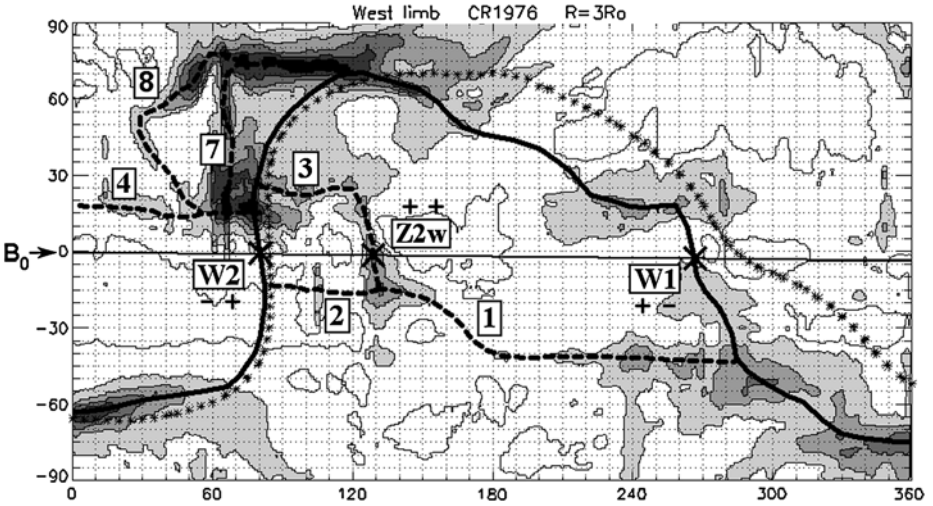

Figure 2 Same as Figure 1 but based on the W-limb observation.

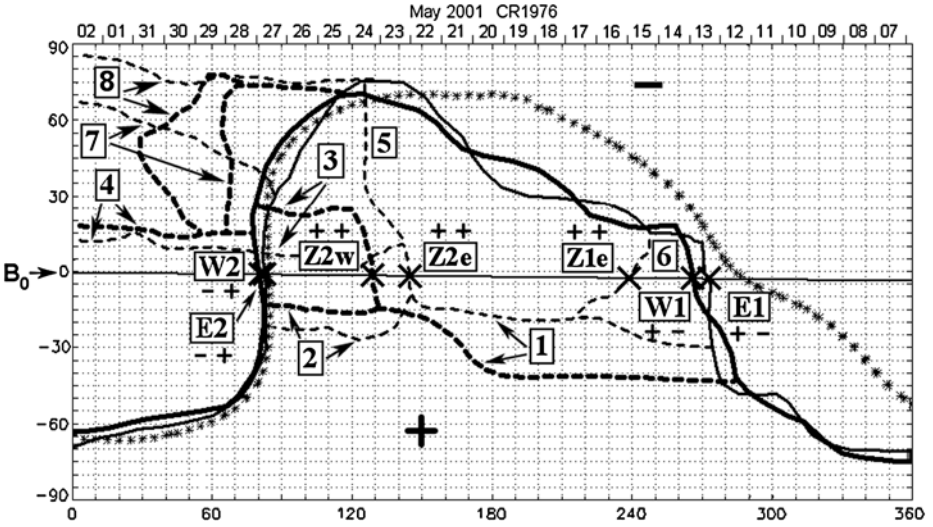

Figure 3 Locations of both the belt and chains of streamers based on observations of both limbs. Designations are the same as in Figures 1 and 2. Thin lines are E-limb data and thick lines are W-limb data.

Chains of streamers are less stable structures in comparison with the streamer belt. It is seen in Figure 3 that chains with numbers 1 – 4 were registered on both limbs, although they underwent changes in form and position in longitude and latitude within $\approx \pm(10-50)$ degrees. In place of chains 7 and 8 observed on the E limb, two new chains appeared on the W limb (denoted as 7 and 8, too). This means that the life-time of such chains is less than 14 days at least. Chains 5 and 6 were registered only on the E limb.

Let us compare intersections (shown by crosses) of the belt and chains of streamers with the ecliptic (the horizontal straight line labeled B_0 in Figures 1 – 3) to their manifestations at Earth's orbit. The streamer belt has two such intersection points: point 1 (longitudinal positions of that point are different according to observations on the E and W limbs and are denoted respectively E1 and W1), and point 2 (E2 and W2). (The plus and minus signs indicate the direction of the radial component of the global magnetic field to the left and right of the intersection point.) The chains also have two intersection points as evident from observation on the W and E limbs. They are denoted as (Z1e, Z2e) and Z2w, respectively (the first point is absent from the W-limb observation).

Using the transit time of 5.5 days (see Section 3) one can get the arrival time of these points to Earth's orbit. Figure 4 shows the time dependence of the density N, velocity V, the azimuth angle of magnetic field φ in GSE system, and the entropy argument $T/N^{0.5}$ for the solar wind at Earth's orbit according to OMNI2 data having one-hour resolution. WIND data are shown as thin lines in Figure 4 for a few time intervals for which OMNI2 density data were lacking.

The calculated moments of the arrival of the intersection points between the streamer and chains of streamers at 1 AU are shown by arrows with respective notations at the bottom of Figure 4. The vertical dashed lines labeled "Streamer" and "Chain" in the top panel of Figure 4 confine the SW intervals which reveal typical values and behavior of parameters $N, V, T/N^{0.5}$ and φ for the belt and chains of streamers. The calculated moments of the arrival of the points (E1, W1) and (E2, W2) at 1 AU coincide with the "Streamers" intervals at Earth's orbit, while the arrival times of points Z1w and Z2e,w coincide with the "Chain" intervals with an accuracy of ± 1.5 days. Note that the chain near May 28 – 29 is disturbed by a sporadic stream triggering the storm sudden commencement (SSC) on May 27 14:59 (shown by an upturned triangle in Figure 4).

We correlated the position of the belt and chains of streamers for CR1976 with SW velocity contours obtained by the IPS method. To do this, we plotted the position of the belt and chains constructed based on the E-limb brightness of the corona onto a synoptic map of SW velocity contours on the source surface (Figure 5). It is seen in the figure that, within an uncertainty of $\pm(20-30)$ degrees in longitude and latitude, the streamer belt is largely situated in the region of minimum SW velocities $V < 450-550$ km s^{-1} (it is the darkest region in the map). It should be noted that the positions of the streamer belt and SW velocity distribution on the synoptic map were obtained by means of different techniques, with different averaging methods employed. A typical averaging time in both cases is large enough and comparable with the time of one rotation of the Sun. The same is true for the chains: their positions generally also avoid regions with high SW velocity. On the whole, the belt and chains of streamers obviously constitute a "network" that encircles high-velocity regions and is positioned in low-velocity regions.

Figure 6 shows distributions of velocity occurrence along the streamer belt and chains of streamers based on the IPS map. The points were taken at 1-degree intervals along the streamer belt for the distribution in the top panel of Figure 6, and along all seven chains in Figure 5 for the distribution in the bottom panel of Figure 6. Obviously, most points belonging to the belt and chains of streamers lie within the range of the slow SW ($V < 450$ km s^{-1}).

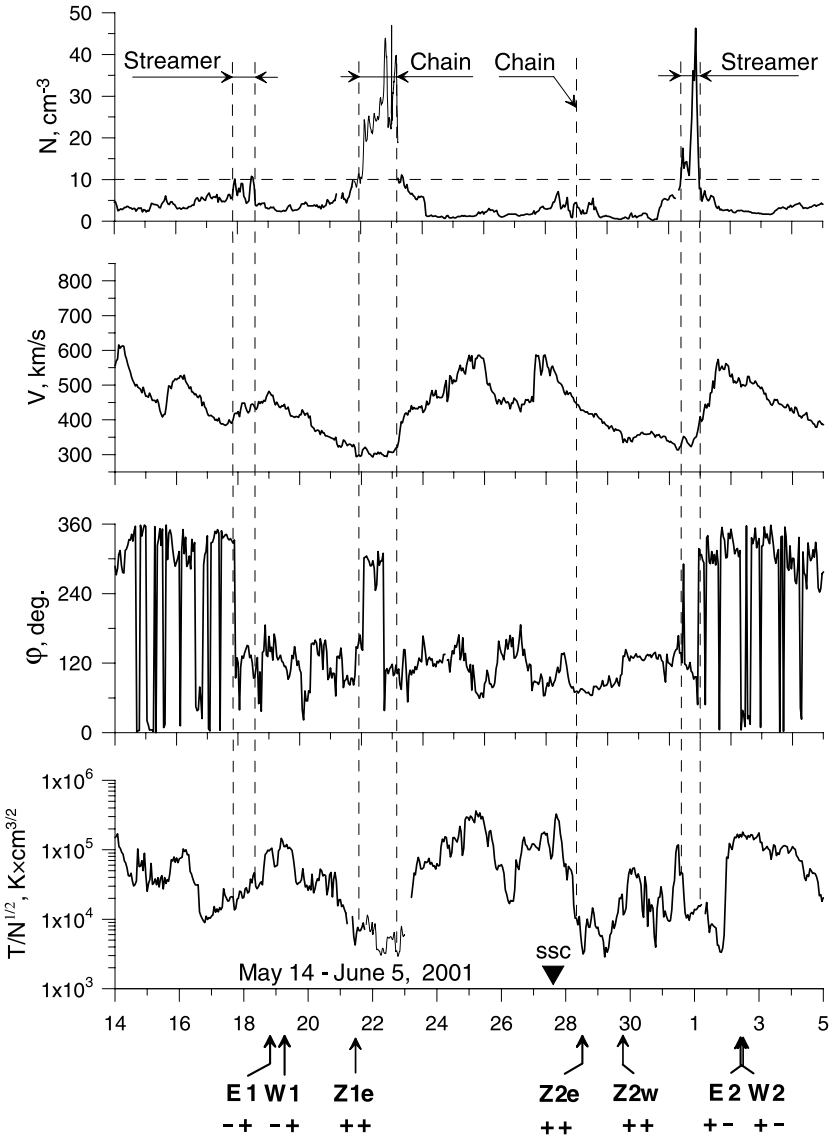

Figure 4 Solar wind parameters at Earth's orbit from May 14 to June 5, 2001 (OMNI2 data). Density data for May 21 – 22, 2001 are from WIND with about 1-minute time resolution.

Along the streamer belt, 67%, and along the chains, 85%, of points have velocities less than 450 km s^{-1}. The total length of the chains in the CR1976 rotation was smaller than or comparable to the length of the streamer belt. The chains were even situated at latitudes as high as 70 – 80 degrees.

Let us consider (in less detail) the CR1963 rotation (May 17 – June 13, 2000) as another example containing very long high-latitude chains. Figure 7 shows a synoptic map of coronal brightness according to LASCO data on the W limb (at $R = 3R_0$) with positions of the belt

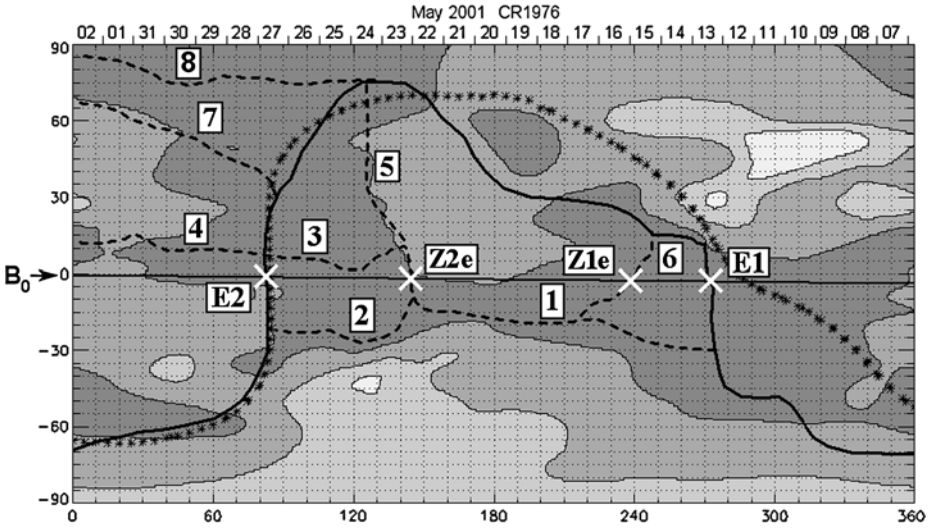

Figure 5 Synoptic map of SW velocity for the CR1976 rotation based on IPS measurements. Dark-to-light brightness levels correspond to velocities 300, 450, 600, and 700 km s^{-1}. The positions of the streamer belt, chains, and NL are coded as in Figure 1.

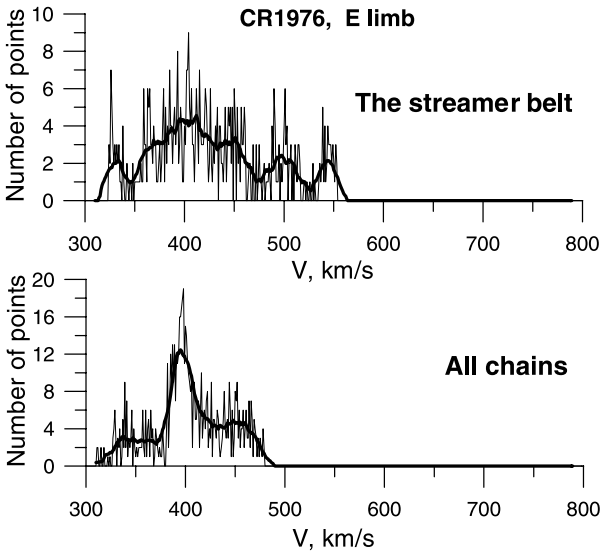

Figure 6 Distributions of velocity occurrence for CR1976: top panel — along the streamer belt; bottom panel — along all the chains of streamers. Based on IPS velocity data.

and chains of streamers plotted on. We took into account the fact that, in the longitude range of 180 – 270 degrees, a stable CH existed near the equator, but there was no north polar coronal hole. At longitudes of 60 – 100 degrees, there was a CH between chains 1 and 2, and, possibly, an unstable polar CH was present. High-latitude chains 3 and 4 appeared to continue on the other side of the Sun.

The belt and chains constructed in this way were plotted onto the SW velocity map according to IPS data and are shown in Figure 8. The chains occupy nearly all latitudes up

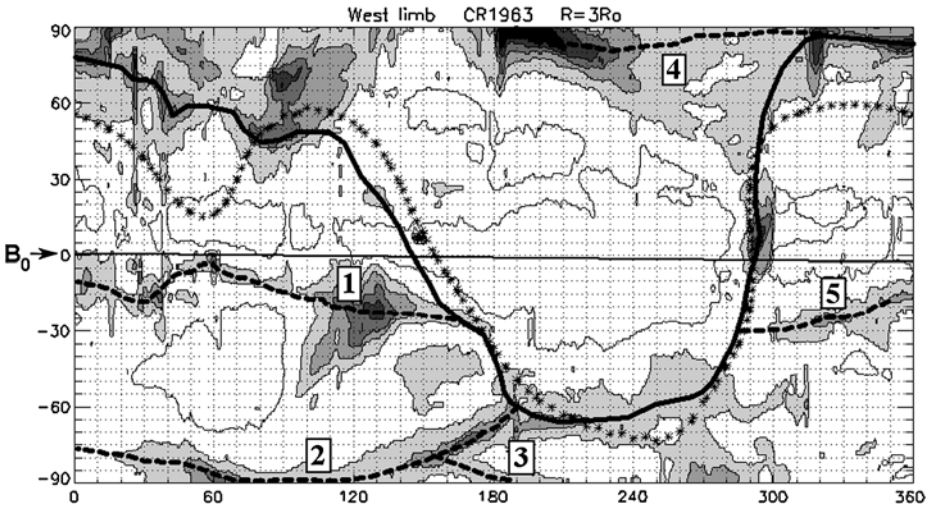

Figure 7 Contours of white-light coronal brightness on a synoptic map. Based on LASCO C2 data for W limb, $R = 3R_0$, CR1963. Designations are the same as in Figure 1.

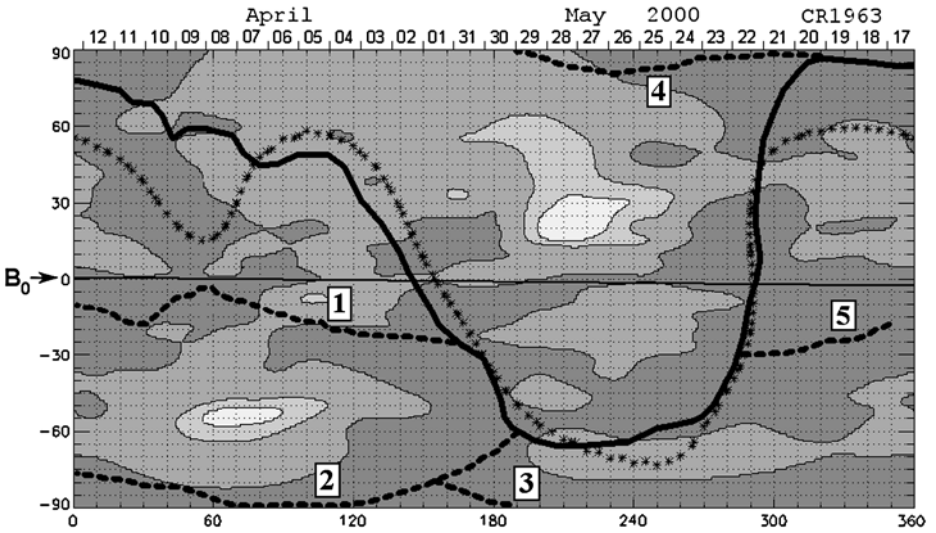

Figure 8 Synoptic map of SW velocity for the CR1963 rotation based on IPS measurements. Dark-to-light brightness levels correspond to velocities 300, 450, 600, and 700 km s^{-1}. The positions of streamer belt, chains, and NL are coded as in Figure 7.

to ±90 degrees and the total length of the chains is comparable to the streamer belt length as is evident from the figure. The streamer belt replicates fairly well the NL profile and runs mainly through regions with SW velocities <450 km s^{-1}. Chains 1 and 2 appear to run around high-velocity regions and are situated basically in regions with $V < 450$ km s^{-1}. Chains 3, 4, and 5 exhibit the same behavior.

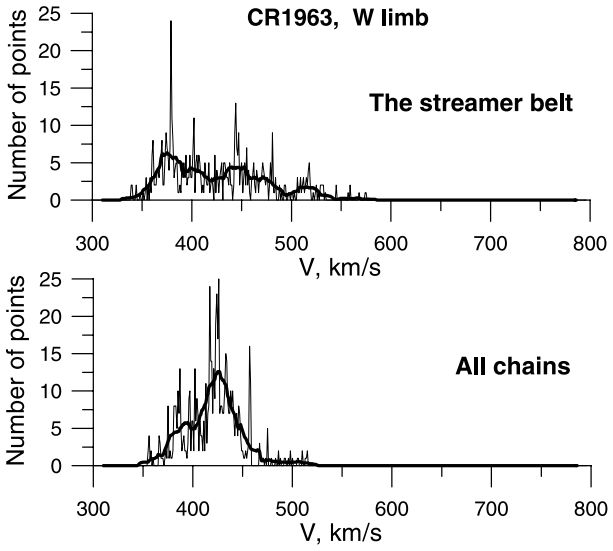

Figure 9 Same as Figure 6 but for CR1963.

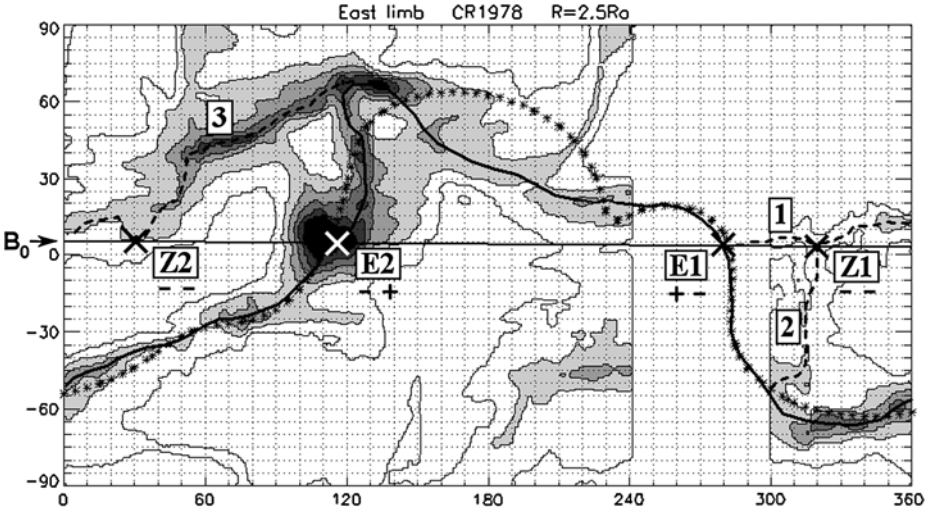

Figure 10 Same as Figure 7 but for CR1978 (E limb, $R = 2.5R_0$).

Figure 10 shows distributions of velocity occurrence in the synoptic map along the streamer belt (Figure 10, top panel) and chains of streamers (Figure 10, bottom panel). Obviously, most points of the belt and chains of streamers lie within the range of the slow SW ($V < 450$ km s^{-1}). Such points make up 70 and 89%, for the streamer belt and chains, respectively.

The two examples that we have examined provide convincing evidence that the streamer belt and chains of streamers are sources of the slow SW with high density. As a source of slow SW, chains can be responsible for a fraction comparable to that of the streamer belt.

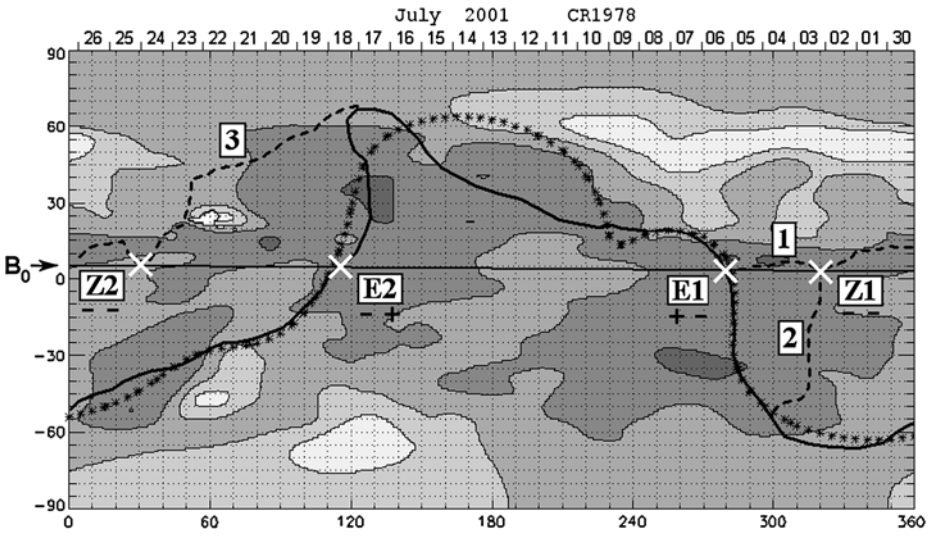

Figure 11 Same as Figure 8 but for CR1978.

5. Intersections of Chains with the Ecliptic and Their Manifestations at Earth's Orbit

In the CR1963 case, there are no intersections of chains with the ecliptic plane whereas the streamer belt intersects the ecliptic twice. Comparison of the parts of chains that intersect the ecliptic and their manifestations at Earth's orbit may serve as additional important evidence that the chains are sources of slow SW. Let us consider two more examples in which only chains intersecting the ecliptic plane stand out. For this purpose, we select those cases where parts with increased brightness (plasma density) are located near the ecliptic plane. This ensures that the given part of the chain be registered at Earth's orbit.

CR1978 (June 30 – July 27, 2001). The map of white-light coronal brightness on the E limb ($R = 2.5R_0$) has a data gap at longitudes 240 – 300 degrees (see Figure 10). Therefore the streamer belt (solid curve) in this longitude range is plotted along the calculated neutral line (asterisks). Two chains (dashed curves) closely approach the ecliptic and possibly intersect it at points Z1 and Z2 at least. The streamer belt intersects the ecliptic at points E1 and E2.

One can see from the velocity synoptic map in Figure 11 that the streamer belt and the chain with the intersection point Z2 avoid regions with maximum velocities, and the whole of the chain with the intersection point Z1 is situated in a region with minimum velocities $V < 450\ \mathrm{km\,s^{-1}}$.

The calculated times of arrival of the intersection points of the belt (E1, E2) and chains (Z1, Z2) at 1 AU are marked by arrows with respective designations at the bottom of Figure 12. Intervals corresponding to manifestations of the belt and chains of streamers at Earth's orbit are shown by vertical dashed lines (labeled "Streamer" and "Chain" in the top plot in Figure 12).

CR1948 (April 4 – May 1, 1999). On the white-light coronal brightness map (W limb, $R = 5R_0$) in Figure 13, chain 1 and chain 2 have each one intersection point with the ecliptic (Z1 and Z2, respectively), and the streamer belt has three intersection points — W1, W2 and W3. On the velocity map in Figure 14 the belt and chains of streamers generally avoid regions with large velocities.

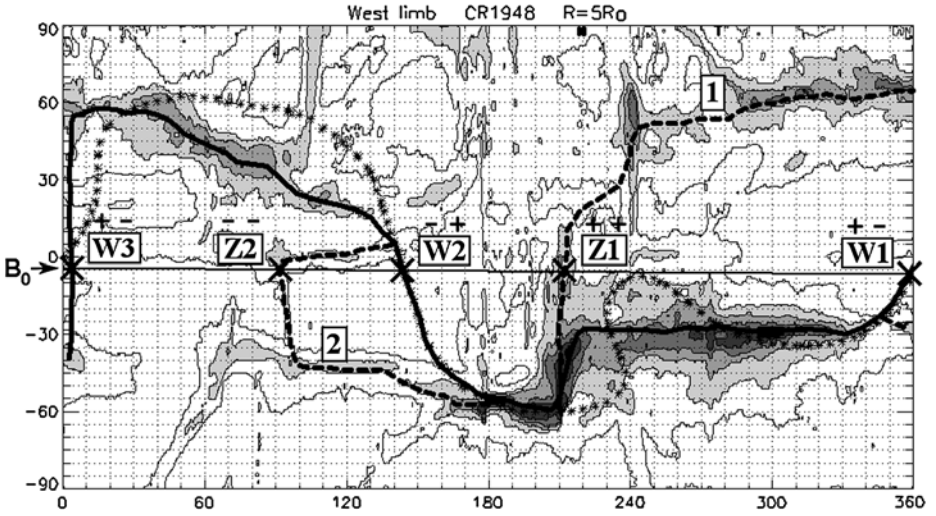

Figure 12 Solar wind parameters at Earth's orbit from July 6 to August 2, 2001 (OMNI2 data). Density data for July 8, 9, 12, August 29, 30 (2001) are from WIND with about one-minute time resolution.

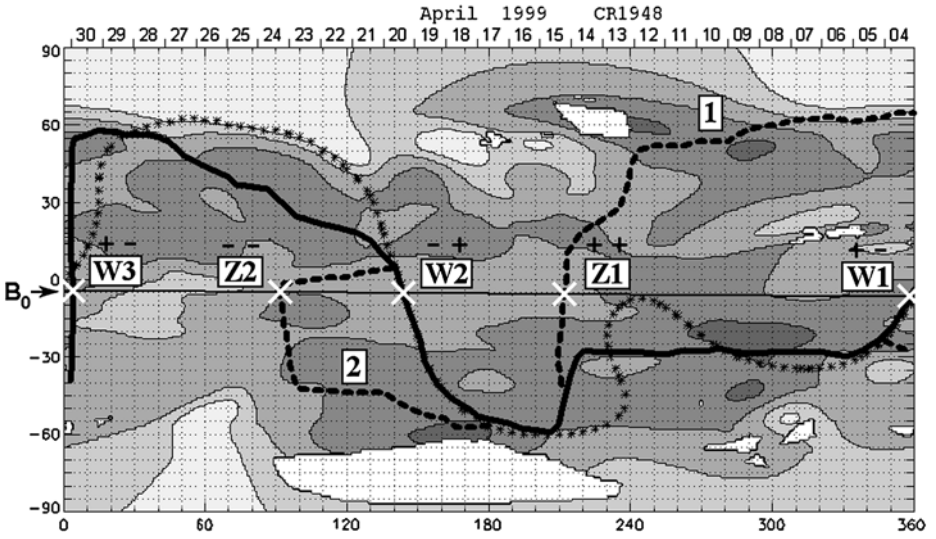

Figure 13 Same as Figure 7 but for CR1948 (W limb, $R = 5R_0$).

The calculated times of arrival of the intersection points of the belt (W1, W2 and W3) and chains (Z1 and Z2) at 1 AU are marked by arrows with respective designations at the bottom of Figure 15. During this Carrington rotation, at least two sporadic streams (associated with two SSC, on April 16 11:25 and May 5 15:43) were observed at Earth's orbit. The former stream could disturb the part of the chain of streamer (Z1), while the latter the part of the streamer belt (W3), at Earth's orbit.

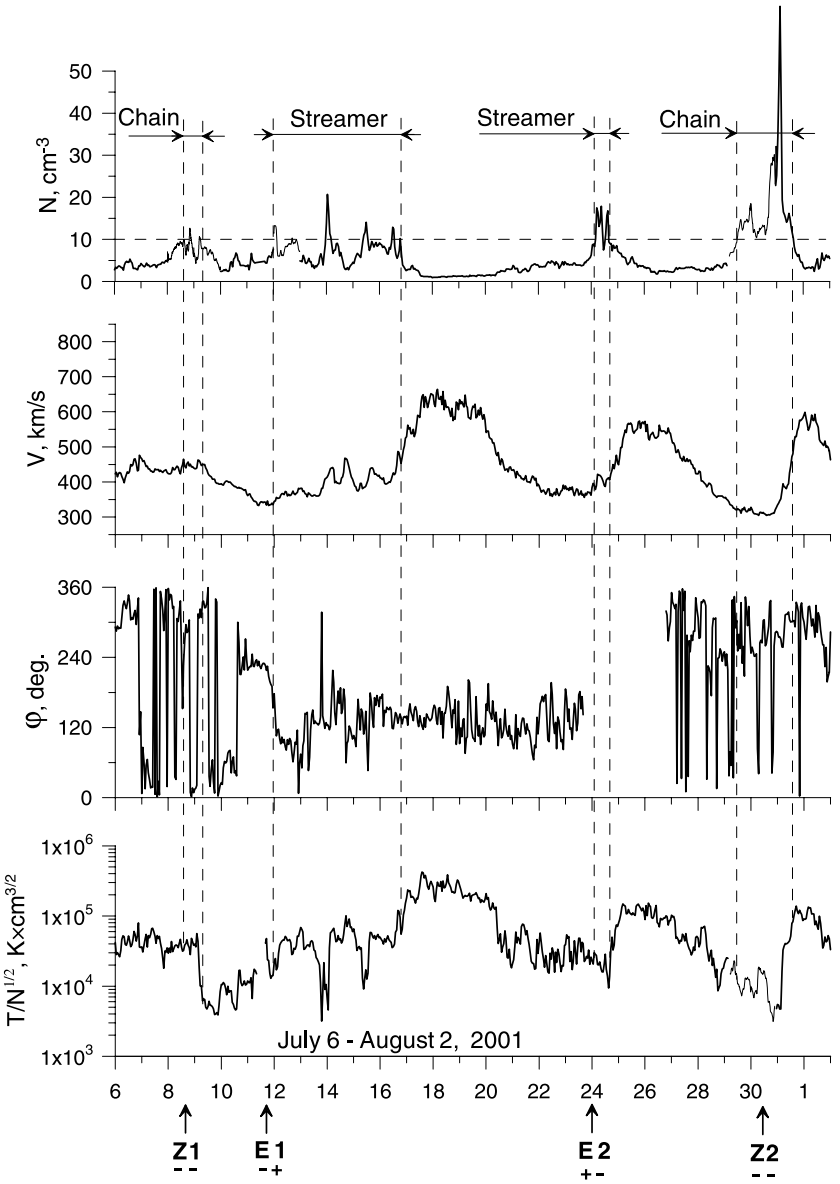

Figure 14 Same as Figure 8 but for CR1948.

6. Discussion

A comparison of coronal brightness synoptic maps and SW velocity maps obtained from IPS for the rotations CR1976 and CR1963 has shown that the majority of sources of slow SW with increased density and velocity $V < 450$ km s^{-1} are localized in the streamer belt and chains of streamers. At the same time, the contribution to the slow SW from the chains of streamers may be comparable to that from the streamer belts. The parts of chains and belt

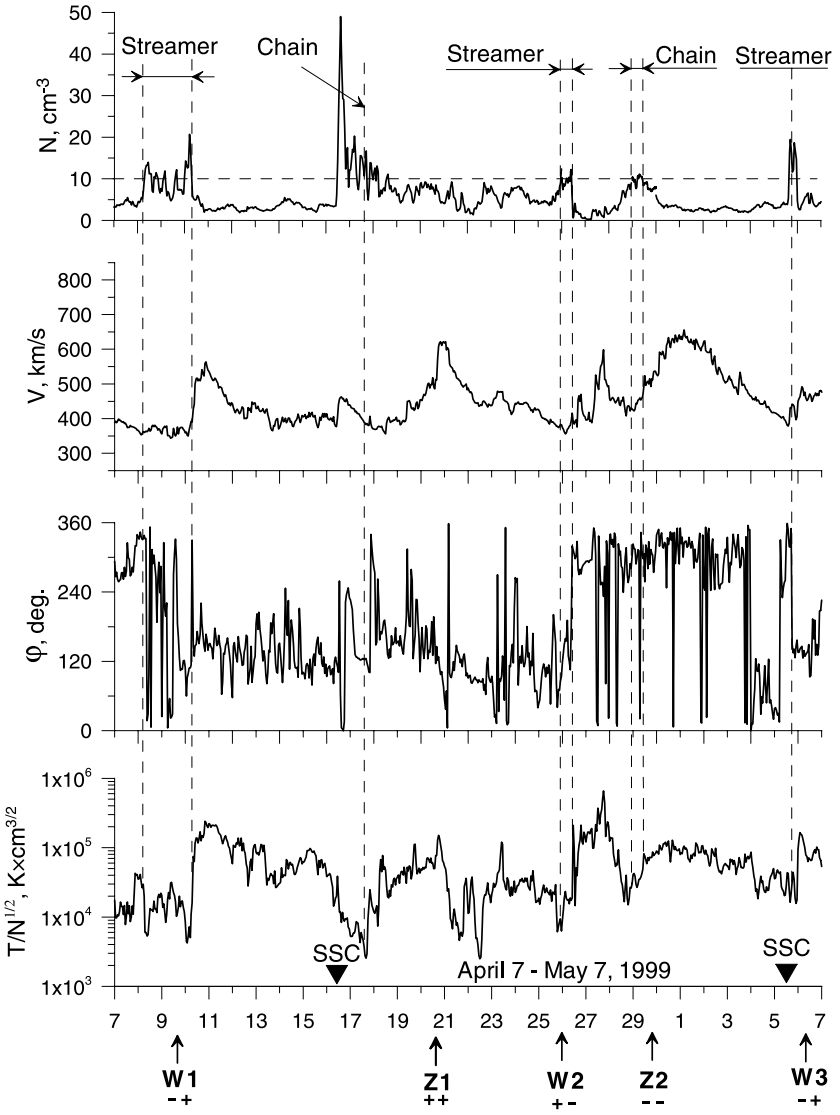

Figure 15 Solar wind parameters at Earth's orbit from April 7 to May 7, 1999 (OMNI2 data). Density data for April 25, 26, 29, 30 are from WIND with about one-minute time resolution.

of streamers intersecting the ecliptic arrive at Earth's orbit about 5 days later as was shown on the example of the rotations CR1976, CR1978, and CR1948.

The parts of chains of streamers of May 22, 2001 (CR1976, Figure 4), July 30 – 31, 2001 (CR1978, Figure 12), and April 29, 1999 (CR1948, Figure 15) have a "classic" appearance at Earth's orbit. They look like parts of the streamer belt, with one exception: there is no sector boundary within them. The azimuth angle of magnetic field shows an even number of changes and IMF sign is the same on each side of that part.

Near the maximum solar activity phase (to which the rotations under study correspond), parts of chains (and the belt) of streamers with somewhat increased velocity (near 450 km s^{-1}) and entropy $T/N^{0.5} \leq 5 \times 10^4$ K $cm^{3/2}$ (but less than in fast SW) often appear. The chains on July 8 – 9, 2001 (CR1978, Figure 12), April 29, 1999 (CR1948, Figure 15), and the streamer belt on May 17 – 18, 2001 (CR1976, Figure 4) are such parts. Typical plasma parameters in the streamer belt of May 5 – 6, 1999, the chain of April 17 – 19, 1999 (CR1948, Figure 15), and the chain of May 28, 2001 (CR1976, Figure 4) are, possibly, disturbed by sporadic streams of SW.

7. Conclusion

A comparison of coronal brightness distributions with SW velocity distributions obtained from IPS has given evidence that the streamer belt and chains are the main sources of the slow SW with increased density and decreased entropy. At the same time, the contribution to the slow SW from the chains of streamers may be comparable to that from the streamer belt.

Acknowledgements The SOHO/LASCO data used here were produced by a consortium of Naval Research Laboratory (USA), Max-Planck-Institut für Aeronomie (Germany), Laboratoire d'Astronomie (France), and the University of Birmingham (UK). SOHO is a project of international cooperation between ESA and NASA. Wilcox Solar Observatory data used in this study were obtained via the website http://quake.stanford.edu/~wso courtesy of J.T. Hoeksema. We are grateful to K.W. Ogilvie (NASA GSFC), A.J. Lazarus (MIT), and M. R. Aellig (MIT) for making the WIND/SWE data available. We would like to thank NASA/Goddard Space Flight Center for providing OMNI 2 data. Finally, we thank the referee for helpful comments that improved this paper.

References

Borrini, G., Wilcox, J.M., Gosling, J.T., Bame, S.J., Feldman, W.C.: 1981, *J. Geophys. Res.* **86**, 4565.
Brueckner, G.E., *et al.*: 1995, *Solar Phys.* **162**, 357.
Burlaga, L.F., Hundhausen, A.J., Zhao, X.P.: 1981, *J. Geophys. Res.* **86**, 8893.
Burton, M.E., Neugbauer, M., Crooker, N.U., von Steiger, R., Smith, E.J.: 1999, *J. Geophys. Res.* **104**, 9925.
Eselevich, M.V., Eselevich, V.G.: 2005, *Geomagnetizm i Aeronomiya* **45**, 347 (English translation: *Geomagnetism and Aeronomy* **45**, 326).
Eselevich, V.G., 1995, *Geophys. Res. Lett.* **22**(20), 2681.
Eselevich, V.G., Eselevich, M.V.: 1999, *Solar Phys.* **188**, 299.
Eselevich, V.G., Eselevich, M.V.: 2002, *Solar Phys.* **208**, 5.
Eselevich, V.G., Fainshtein, V.G.: 1992, *Planet. Space Sci.* **40**, 105.
Eselevich, V.G., Fainshtein, V.G., Eselevich, M.V.: 2000, *Solar Phys.* **200**, 259.
Eselevich, V.G., Fainshtein, V.G., Rudenko, G.V.: 1999, *Solar Phys.* **188**, 277.
Eselevich, V.G., Kaigorodov, A.P., Fainshtein, V.G.: 1990, *Planet. Space Sci.* **38**, 459.
Eselevich, V.G., Tong, Y.: 1997, *J. Geophys. Res.* **102**, 4681.
Fainshtein, V.G.: 1999, Properties of the Solar Wind Streams and Their Sources. Ph.D. Thesis, Institute of Solar-Terrestrial Physics, Irkutsk.
Geiss, J., Gloeckler, G., von Steiger, R.: 1995, *Space Sci. Rev.* **72**, 49.
Gosling, J.T., Borrini, G., Asbridge, J.R., Bame, S.J., Feldman, W.C., Hansen, R.T.: 1981, *J. Geophys. Res.* **82**, 5438.
Ivanov, K., Bothmer, V., Cargill, P.J., Kharshiladze, A., Romashets, E.P., Veselovsky, I.: 2002, In: Wilson, A. (ed.) *Solar Variability from Core to Outer Frontiers, ESA SP-506*, p. 141.
Korzhov, N.P.: 1977, *Solar Phys.* **55**, 505.
Kojima, M., Fujiki, K., Ohmi, T., Tokumaru, M., Yokobe, A., Hakamada, K.: 1999, *J. Geophys. Res.* **104**, 16993.
Kojima, M., *et al.*: 1998, *J. Geophys. Res.* **103**(A2), 1981.
McComas, D.J., Elliott, H.A., von Steiger, R.: 2002, *Geophys. Res. Lett.* **29**, 28-1.

Ohmi, T., Kojima, M., Tokumaru, M., Fujiki, K., Hakamada, K.: 2004, *Adv. Space Res.* **33**, 689.
Sheeley Jr., N.R., *et al.*: 1997, *Astrophys. J.* **484**, 472.
Svalgaard, L., Wilcox, J.M., Duvall, T.L.: 1974, *Solar Phys.* **37**, 157.
Schwenn, R., Marsch, E.: 1991, *Physics of the Inner Heliosphere*, vol. **I**, Springer-Verlag, Berlin.
Smith, E.J., *et al.*: 1993, *Geophys. Res. Lett.* **20**, 2327.
Strachan, L., Suleiman, R., Panasyuk, A.V., Biesecker, D.A., Kohl, J.L.: 2002, *Astrophys. J.* **571**, 1008.
Tappin, S.J., Simnett, G.M., Lyons, M.A.: 1999, *Astron. Astrophys.* **350**, 302.
Wilcox, J.M., Hundhausen, A.J.: 1983, *J. Geophys. Res.* **88**, 8095.
Zhao, X.P., Webb, D.F.: 2003, *J. Geophys. Res.* **108**(A6), SSH4-1.